Preprints of the 21st IFAC World Congress (Virtual)
Berlin, Germany, July 12-17, 2020

Human Decision-Making Behavior Modeling for Human Multi-Robot Interaction System

Wenhua Wu * **Jie Huang**† ** **Zhenyi Zhang** ***

* *College of Electrical Engineering and Automation, Fuzhou University, Fuzhou 350108, China (e-mail: N180127114@fzu.edu.cn).*
** *College of Electrical Engineering and Automation, Fuzhou University, Fuzhou 350108, China (e-mail: jie.huang@fzu.edu.cn).*
*** *College of Electrical Engineering and Automation, Fuzhou University, Fuzhou 350108, China (e-mail: zzyzzy712@163.com).*

Abstract: In this paper, the composition of human decision-making process in human-robot interaction is analyzed and the human decision-making behavior is modeled. The human decision-making process is divided into data-processing station and human cognitive system. By combining with the null-space-based control (NSBC) method, the traditional drift diffusion model (DDM) is applied for for human decision-making behavior modeling in human-robot interaction (HRI). In addition, HRI is studied for a platoon of autonomous robots in an unknown environment with multiple obstacles. Moreover, the human intervention task is designed to help robots achieve tasks successfully. Finally, simulation examples are given to demonstrate the satisfactory performance of the proposed method.

Keywords: Human robot interaction, multi robot system, human drift diffusion model, human decision-making behavior modeling, behavioral control

1. INTRODUCTION

In the past decade, multi-robot system (MRS) has attracted much attention, because it is a loosely coupled robot networks, and the robots in it can solve problems beyond the capability or knowledge of a single robot through interaction. Some achievements on formation control in MRS has been made. The adaptive fuzzy formation control of multiple autonomous agents with prioritized missions is studied (Huang et al., 2019a). The consensus algorithm for first/second order integrator theory and applications is researched (Ren et al., 2008). These studies enrich the application of MRS, and innovative the solutions to problems of MRS.

Thanks to the improved performance and reduced cost, the number of robots in MRS would be freely combined to perform more complex tasks. Whereas, due to the existence of conflicts between tasks, it is sometimes unable to complete the task. Thus, a mechanism for conflicting tasks is needed. The behavioral control is a very effective way to solve this problem. The behavioral-based approach for keeping formation is first proposed and several other behaviors are considered (Balch et al., 2019), but the traditional behavioral control cannot solve task conflict. In this paper, a null-space-based behavioral control (NSBC) is used for a team of autonomous robots, where the priority of the tasks should be configured over the changeable environment (Antonelli et al., 2006). The NSBC architecture is utilized to address the formation control problem of MRS with model uncertainties in the environment (Chen et al., 2016). However, not all conflicts can be solved by NSBC method due to the lack of human supervision and intervention (Goodrich et al., 2008; Huang et al., 2019b).

Therefore, it is necessary to introduce human intervention to achieve HRI in MRS for better control and task performance. So far, the application of HRI has been a hot spot. A framework of HRI in industrial assembly is proposed for the parameter and a state estimation algorithm is presented to optimize a variety of HRI scenarios (Bestick et al., 2015). Besides it, HRI is now applied in many robot tasks, including space, aviation, undersea et al. (Sheridan et al., 2016). To improve the HRI system performance, the human role is indispensable in the field of HRI, which contains active role and supervisory role, the active role means human can provide control input to the subtask, e.g., the trajectory information or velocity command, and the supervisory role means human need to select global behavior, local behavior and intervene robot if necessary, where the global behavior requires information exchange among the robots and the local behavior require only the local information from neighbor robot (Musić et al., 2017).

Although successful in specific applications of interest, the human role aforementioned lack an accurate human model. In HRI system, an appropriate human-decision making model is needed both in the supervisory role and in active role. The human decision-making behavior model in the HRI is within the cognitive psychology, which is the scientific study of mental processes. The cognitive psychology

⋆ This work was supported in part by the National Natural Science Foundation of China under Grant 61603094 (Corresponding Author: Jie Huang).

for human behavior modeling has been researched. A memory theory is applied and a diffusion process is proposed to represent the comparison process of the theory (Ratcliff et al., 1978). After that, the drift diffusion model (DDM) for two-choice decision tasks is proposed for human decision (Ratcliff et al., 2008). The DDM can be cited to account for the accuracy and reaction time of value-based choices for human (Mormann et al., 2010). Additionally, the DDM has been successfully used for human behavior modeling in many human cognitive tasks under social context, e.g., lexical decision (Ratcliff et al., 2004). Comparing to the Markov chain model (Pentland et al., 1999) and the EDFT model (Gao et al., 2006), the DDM does not employ factors such as probability or trust of human but instead uses actual sensory informationin making simple decisions, e.g., two-alternative forced-choicetasks (TAFCTs). Moreover, the human decision-making behavior is rarely modeled by the DDM in the HRI systems. In this paper, the NSBC method is combined with the DDM and obtained the human drift diffusion model (HDDM), which is used for human decision-making behavior modeling.

The contribution of the paper contains two parts:

(1) The composition of human decision-making process in human-robot interaction is analyzed. A data-processing station and human cognitive system is introduced into the human-decision-making process.
(2) The human decision-making process for HRI systems is modeled by the proposed HDDM which combines the traditional drift diffusion model and the NSBC method. We design robot tasks to verify that the human-decision-making process modeling can help robots finish tasks successfully and can provide human decision-making more accurately.

The remainder of the paper is organized as follow: In section 2, the research problem are introduced. In section 3, the robot and human intervention task is designed and the main methodology of prioritized multi-mission composition is presented. Additionally, the HDDM are introduced and the human decision-making behavior is modeled. The simulation is in the section 4.

2. PROBLEM FORMULATION

Consider a group of $n\,(n \geq 2)$ robots with the following model:

$$\dot{p}_j = v_j, \tag{1}$$

where $p_j \in \mathbb{R}^2$ is the position of the robot $j(j = 1, \ldots, n)$, and $v_j \in \mathbb{R}^2$ is the velocity vector. In this paper, we consider a first-order model as in (1) for sake of simplicity. The formation control objective is to make robots follow human instructions and perform tasks, which are defined by different behaviors of robots, e.g., move-to-target and obstacles-avoidance. To decide when to introduce human intervention, we make the following assumption:

Assumption 1: Assuming that robots are completely autonomously controlled, the human intervention can only happen when the controller of the robots fail to finish tasks.

3. TASK DESIGN AND COMPOSITION

3.1 Move-to-target Task Function Design

The behavior which drives the robots team to the target points $p_{gj} = [\, x_{gj} \; y_{gj} \,]^T$. Once each robot arrive at the target point, the team would stop. Thus, the behavior corresponding to the move-to-target task of the jth robot is encoded by the task function ρ_{mj}:

$$\rho_{mj} = p_j \tag{2}$$

where p_j is the jth robot position, and the desired function ρ_{mdj} is:

$$\rho_{mdj} = p_{gj} \tag{3}$$

The output of the function is encoded by the NSBC method:

$$v_{mj} = J_{mj}^{\dagger} \left(\dot{\rho}_{mdj} + \Lambda_{mj} \tilde{\rho}_{mj} \right) \tag{4}$$

where Λ_{mj} is denoted the positive constant of gains of move-to-target task, $\tilde{\rho}_{mj} = \rho_{mdj} - \rho_{mj}$ is the task error, $J_m j$ is the configuration-depending task Jacobian matrix, and $J_{mj}^{\dagger}$ is the pseudo-inverse of J_{mj}.

3.2 Obstacles-Avoidance Task Function Design

In presence of an obstacle in the advancing direction, its aim is to keep the robot on a safe distance from the obstacle. D is defined as the radius of the circular safety area. Once the obstacles are within the safety area of robots, the robots must execute the obstacles-avoidance behavior. Thus, the obstacles-avoidance behavior is defined as follows:

$$\rho_{aj} = \| p_j - p_{oj} \| \, , \rho_{adj} = D \tag{5}$$

where ρ_{aj} is the function of obstacles-avoidance task and p_{oj} is the obstacle position of the jth robot. ρ_{adj} is defined as the desired obstacles-avoidance function. Then the velocity output of obstacles-avoidance task is given by:

$$v_{aj} = J_{aj}^{\dagger} \left(\dot{\rho}_{adj} + \Lambda_{aj} \tilde{\rho}_{aj} \right) \tag{6}$$

where Λ_{aj} is the positive constant of gains, the task error $\tilde{\rho}_{aj} = \rho_{adj} - \rho_{aj}$, and the pseudo-inverse of the Jacobian matrix J_{aj} is $J_{aj}^{\dagger} = J_{aj}^T \left(J_{aj} J_{aj}^T \right)^{-1}$.

3.3 Human Decision-Making Behavior Modeling

In this paper, the human decision-making behavior is a process in which one behavior is chosen from a set of human behaviors, and this behavior can help robots team finish tasks successfully. As previous description, the human decision-making behavior can be modeled by adopting the DDM. In Fig.1, the decision making schematic diagram under human intervention is constructed, in which the data procession station and human cognitive system are introduced. The data information related to the progress of task execution is transported to the data processing station, and it would be divided into multi parts. The DDM can translate the data information into components of human decision-making information, but not all data information is used to support human makes decision, e.g., ρ_{aj}. In this paper, the trajectory error $\tilde{p}_j$ of the jth robot, which is the difference between robot reference trajectory from NSBC and robot preset trajectory, is the selected information. The drift rate is denoted as the velocity error

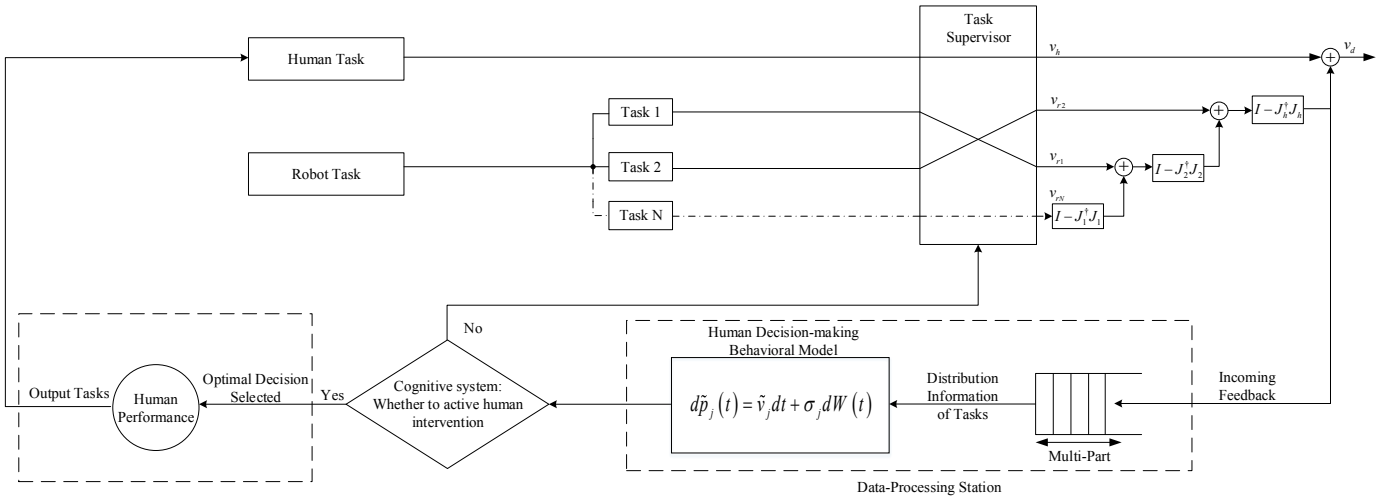

Fig. 1. The decision making schematic diagram under human intervention during task execution

$\tilde{v}_j$, which represents the amount of change in $\tilde{p}_j$ per unit of time (Ratcliff et al., 1998). Thus, the formula of HDDM based on $\tilde{p_j}$ is designed as following:

$$d\tilde{p}_j(t) = \tilde{v}_j dt + \sigma_j dW(t) \tag{7}$$

where $\tilde{p}_j = p_{rdj} - p_j$, and it supports human decision-making on the jth robot, where p_{rdj} and p_j are the robot preset trajectory and robot reference trajectory from NSBC of the jth robot at time t, respectively. $d\tilde{p}_j$ denotes the change in $\tilde{p}_j$ over a unit time internal dt. It contains two parts, the first part is that the amount change in information per time is $\tilde{v}_j$. $\tilde{v}_j = v_{dj} - v_j$ is the drift rate, which is time varying value. In the task execution process, it is the velocity difference. v_{dj} is the velocity related to the preset trajectory and v_j is reference velocity that is obtained from NSBC. $W(t)$ is standard Wiener process (Hitsuda et al., 1968), σ_j is standard deviation of the noise on the jth robot.

As shown in Fig.1, the human decision-making behavior model is designed, and the human makes decisions among the finite set of behaviors, which contains supervision behavior and intervention behavior. In the HDDM, the behavior is only to be chosen or not to be chosen. Additionally, it is noted that the human can only choose one behavior at each unit time. In HDDM equation (7), the selected information for human decision-making $\tilde{p}_j$ evolves over time , and when it is equal to some value, which is called threshold, the human should make decision. The HDDM in this paper is studied in free response paradigm. In this paradigm, the human makes decision until the evidence passes through the preset threshold for the first time, which means the amount of selected information required to trigger a decision response (Peters et al., 2015). Thus, the key to accurately decision-making is the setting of the threshold. The optimal threshold for HDDM is derived by minimizing the Bayes Risk (BR), which is a common criteria to capture speed-accuracy trade-off (Edewards et al., 1965). Thus, the formula of BR is given as following:

$$B = c_{1j}T_j + c_{2j}E_j \tag{8}$$

where B is a cost function of BR, c_{1j} and c_{2j} are the observing cost per unit time in decision-making process and cost of decision-making error, respectively. j is the number of robot, T_j and E_j are the decision time and the error rate, which are given by the following equations (Bogacz et al., 2006):

$$E_j = \frac{1}{1+e^{2\bar{\varsigma}_j \bar{a}_j}} - \left(\frac{1-e^{-2\tilde{p}_{0j}\bar{a}_j}}{e^{2\bar{\varsigma}_j\bar{a}_j} - e^{-2\bar{\varsigma}_j\bar{a}_j}}\right) \tag{9}$$

$$T_j = \bar{\varsigma}_j \tanh(\bar{\varsigma}_j \bar{a}_j) + \left(\frac{2\bar{\varsigma}_j\left(1-e^{-2\tilde{p}_{0j}\bar{a}_j}\right)}{e^{2\bar{\varsigma}_j\bar{a}_j} - e^{-2\bar{\varsigma}_j\bar{a}_j}} - \tilde{p}_{0j}\right), \tag{10}$$

where $\bar{\varsigma}_j = \frac{\varsigma_j}{\tilde{v}_j}$ and $\bar{a}_j = \left(\frac{\tilde{v}_j}{\sigma_j}\right)^2$. To obtain the threshold for HDDM, the equation (9) and (10) are substituted into the equation (8), then differentiating with respect to ς_j and the cost function B is minimized to 0, which yields the equation related to the human decision threshold ς_j:

$$\begin{aligned} &C_j\left[\frac{-2\bar{\varsigma}_j e^{2\vartheta}}{(1+e^{2\vartheta})^2} - \frac{\left(e^{-2\tilde{p}_{0j}\bar{a}_j}-1\right)\left(2\bar{a}_j e^{2\vartheta}+2\bar{a}_j e^{-2\vartheta}\right)}{\left(e^{2\vartheta}-e^{-2\vartheta}\right)^2}\right] \\ &+\left[(\tanh(\vartheta)+\bar{a}_j) + \frac{2\left(1-e^{-2\tilde{p}_{0j}\bar{a}_j}\right)\left(e^{2\vartheta}-e^{-2\vartheta}\right)}{\left(e^{2\vartheta}-e^{-2\vartheta}\right)^2}\right] \\ &+\frac{(1-2\vartheta)}{\left(e^{2\vartheta}-e^{-2\vartheta}\right)^2} = 0 \end{aligned} \tag{11}$$

where $\vartheta = \bar{\varsigma}_j \bar{a}_j$, and $C_j = \frac{c_{2j}}{c_{1j}}$.

After determining the threshold, once $\tilde{p}_j$ evolves and crosses the threshold for the first time, human operator should choose behavior among the finite behavior space. The monitor behavior is the human supervisors the robot task execution process, and there is no task input to the robots, but the human intervene behavior would provides input to the robots. Thus, the human intervention task should be designed.

3.4 Human Intervention Task Design

If the optimal decision is human intervention behavior, then the human intervention task is designed and is input to the supervisor. The human intervention task is set the

highest priority and the original robots task would be turned into the lower priority. The human intervention task is similar to robot tasks, which can be identified by robots. The human intervention task function is defined as following:

$$\rho_h = f(p_h) \tag{12}$$

where $\rho_h \in \mathbb{R}^m$ and m is the dimension of the task space. f is the differentiable function. p_h is the position of the robot that the human would intervene.

Then the differential of the human intervention task is:

$$\dot{\rho}_h = \frac{\partial f(p_h)}{\partial p_h}\dot{p}_h = J_h v_h \tag{13}$$

where $J(h) \in \mathbb{R}^{m\times 1}$ is the configuration-dependent behavior Jacobian matrix, and it represents the mapping between ρ_h and p_h. Through inverting the mapping, a typical requirement is to pursue minimum-norm velocity and leading to:

$$v_h = J_h^{\dagger}\left(\dot{\rho}_{hd} + \Lambda_h \tilde{\rho}_h\right) \tag{14}$$

where Λ_h is the positive constant of gains in human intervention task and the human intervention task error $\tilde{\rho}_h = \rho_{hd} - \rho_h$, $J_h^{\dagger}$ is the pseudo-inverse of J_h. In this paper, when multi tasks are considered, as shown in the Fig.1, if human intervention task existed, then the original robot task vector should project onto the null space of human intervention task, and it ensures the complete execution of human intervention tasks, the contradictory parts of robot tasks are cleared so as to perform the non-contradictory parts of task.

3.5 Task Priority Design

In task execution process, the task priority should be designed. The low priority task should project onto the null-space of the high priority task. In general, the obstacles-avoidance task is set the high priority. Thus, one can obtain the final output velocity command of the robots:

$$v_{rj} = v_{aj} + \left(I - J_{aj}^{\dagger}J_{aj}\right)v_{mj} \tag{15}$$

where v_{rj} is the velocity output of robot task, and j is the number of robots. $I - J_{aj}^{\dagger}J_{aj}$ is the null space of the obstacles-avoidance task.

The human intervention task is set the highest priority within task execution process, and the integration diagram of human intervention tasks and robot tasks is shown in the following:

$$v_j = v_h + \left(I - J_h^{\dagger}J_h\right)v_{rj} \tag{16}$$

where $I - J_h^{\dagger}J_h$ is the null space of human intervention task.

Remark 1: Human intervention task is similar to the robot task, and it is also the robots identifiable task. By observing the final velocity output by (16), if the null space of human intervention task $I - J_h^{\dagger}J_h = 0$, the robot task cannot be executed simultaneously with human task.

4. SIMULATION

In this section, a platoon of three robots is considered to move in the $x - y$ label plane and each robot is modeled as first-order integration. The initial position of robots are: $p_1 = [1\ 8]^T$, $p_2 = [5\ 6]^T$ and $p_3 = [4\ 1]^T$, respectively. The abostacle position in the coordinate system are: $O_1 = [8\ 11]$, $O_2 = [13\ 10.5]$ and $O_3 = [10\ 4]$. The preset task functions for the robots are: $\rho_{rd1} = [1.4t+2\ \ 0.8t+8]^T$, $\rho_{rd2} = [1.4t+6\ \ 0.8t+6]^T$ and $\rho_{rd3} = [1.4t+5\ \ 0.8t+1]^T$. In the simulation, we defined the safe distance for robots as $1.5m$, the positive constant gain are $\Lambda_{mj} = 15$, $\Lambda_{aj} = 0.8$ and $\Lambda_h = 1.5$. The human decision-making threshold for three robots is all set as $3m$ by the equation (10), where $c_{11} = c_{12} = c_{13} = 0.5$, $c_{21} = c_{22} = c_{23} = 10$, and $C_1 = C_2 = C_3 = 20$, the initial velocity difference for three robots are $\tilde{v}_{0j} = 1$ according to the initial trajectory error, and the diffusion rate for three robots are equaled, where $\sigma_1 = \sigma_2 = \sigma_3 = 1$.

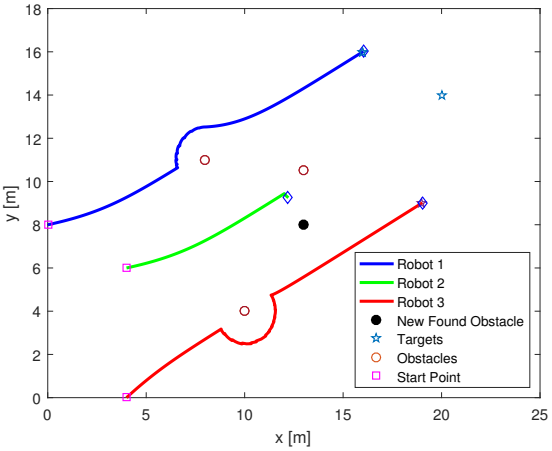

Fig. 2. Trajectory of the three robot in case of unresolved emergency.

4.1 Robot Encounters Local Minima Problem

In this section, robot 1 and robot 3 finish move-to-target task and obstacles-avoidance task autonomously, robot 2 encounter local minima problem while avoiding obstacle, and human intervention behavior is triggered when human decision-making information first reaches the decision threshold. The simulation is shown from Fig. 2 to Fig. 4.

In Fig.2, when the robot 2 is performing obstacle avoidance, the sensor detected a new found obstacle, the distance from new found obstacle and the obstacle which is avoiding are equaled after few seconds, which reflected in the distance from obstacle and new found obstacle are equal to $1.5m$ in Fig.3. Under this situation, the robot 2 encounters local minima problem, which makes the robot unable to move. Under this situation, as shown in Fig.4, the selected information $\tilde{p_j}$ reached the decision-making threshold for the first time at $6.22s$. This time $6.22s$ is the timing of human intervention in this case, the values corresponding to the black solid line and the black dotted line represent the human decision threshold and human decision time, respectively.

4.2 Robot Finishes Tasks with Human Intervention

In this section, the human intervention task is executed by robot 2 after human intervention behavior is triggered,

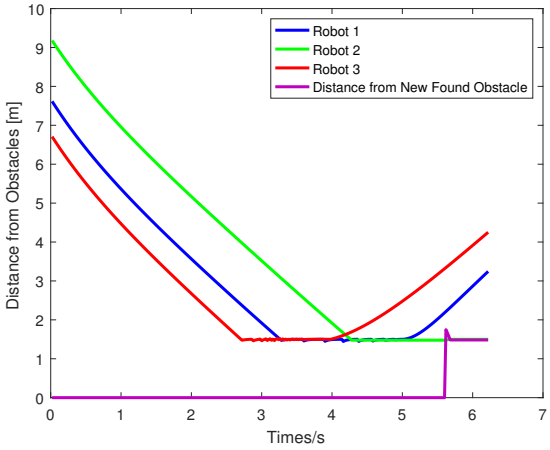

Fig. 3. The distance from obstacles in case of unresolved emergency.

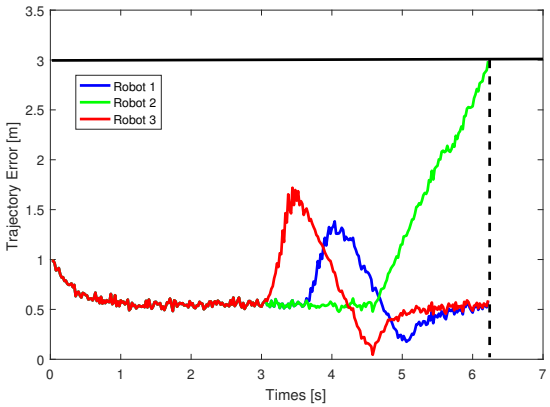

Fig. 4. The trajectory error evolution in case of emergency.

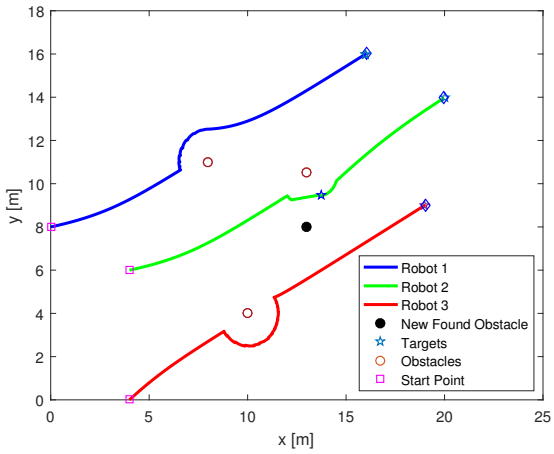

Fig. 5. Robot trajectory diagram under human intervention.

and robot 2 reaches target after human intervention task has been finished. The simulation and response of human intervention task are shown from Fig. 5 to Fig. 8.

Fig. 5 shows human finds the distance between the actual obstacles is larger than the width of the robot itself, then the human give a new targets to the robot, which is

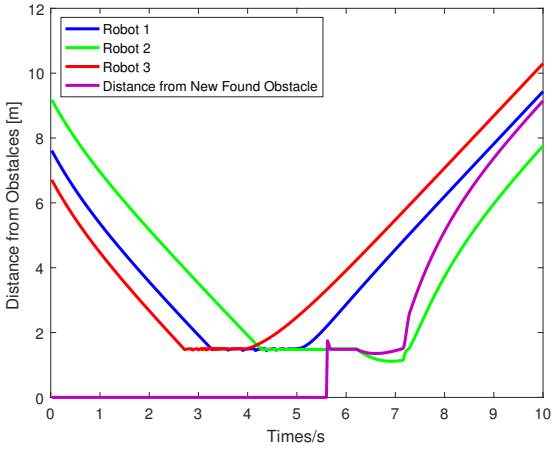

Fig. 6. Distance between robots and obstacles under human intervention.

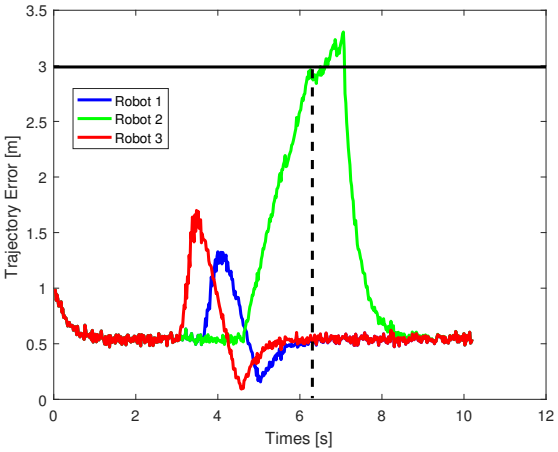

Fig. 7. The trajectory error evolution with human intervention.

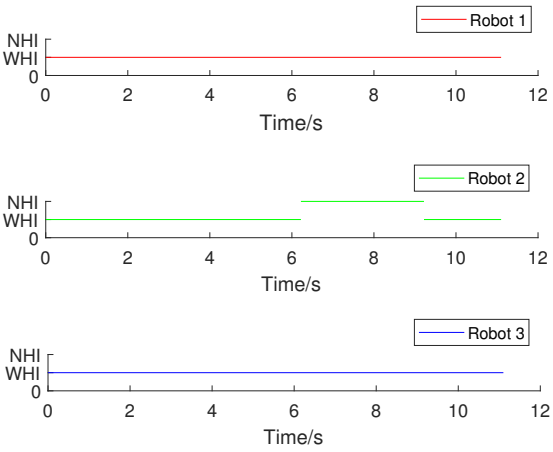

Fig. 8. Responses of the human task. NHI means under human intervention, and WHI means without human intervention.

denoted as an blue pentacle. The human intervention task is set the highest priority, the robot 2 would move to the new targets and escape from local minima point.

As shown in Fig.6, robot 2 passes through the known obstacle and new obstacle to reach new target point $(14m, 9m)$. After that, it activated original robot task and get original targets. Comparing to the traditional control scheme without human intervention (Anonellie et al., 2006), the robot can escape from the local minima point and can reach target successfully. In Fig.7, after human decision making, $\tilde{p}_j$ deceased for the deviation σ_j in HDDM, and increased due to the human decision time and robot execution time, the robot is static. After the robot execute human intervention tasks successfully, the error decreased. In Fig.8, the intervention time location is shown. The robot is intervened by human operator from $6.22s$ to $9.4s$. Except for this time period, the robot relies on the autonomous controller to carry out tasks all the time. The response time of human intervention in the previous work (Fig.8) (Huang et al., 2019b) is not accurate because the timing of intervention does not match that of robot encountering local minima problem. This can be explained by the fact that the timing of human decision-making is simply determined by human experience. In this paper, the robot position error is used as human decision-making information, leading to an exact match of the human intervention timing at local minima problem.

5. CONCLUSION

This paper provides a human decision-making behavior modeling method and extends the control framework for human-robot interaction systems. By combining the drift diffusion model with null-space-based control method, the human drift diffusion model is developed for human decision-making modeling, and the certainly time of human decision is obtained by setting the decision-making threshold. With the human drift diffusion model, the accuracy and speed of human decision-making would be improved. The feasibility of theory is demonstrated by simulations. Our future work is to design the supervisor that is used to switch the defined tasks, and research the HRI based on second-order robots model.

REFERENCES

Antonelli, G., and Chiaverini, S. (2006). Kinematic control of platoons of autonomous vehicles. *IEEE Transactions on Robotics*, 22(6), 1285-1292.

Balch, T., and Arkin, R. C. (1998). Behavior-based formation control for multirobot teams. *IEEE Transactions on Robotics and Automation*, 14(6), 926-939.

Bestick, A. M., Burden, S. A., Willits, G., Naikal, N., Sastry, S. S., and Bajcsy, R. (2015). Personalized kinematics for human-robot collaborative manipulation. *2015 IEEE/RSJ International Conference on Intelligent Robots and Systems*, 1037-1044.

Bogacz, R., Brown, E., Moehlis, J., Holmes, P., and Cohen, J. D. (2006). The physics of optimal decision making: a formal analysis of models of performance in two-alternative forced-choice tasks. *Psychological review*, 113(4), 700-723.

Chen, J., Gan, M., Huang, J., Dou, L., and Fang, H. (2016). Formation control of multiple Euler-Lagrange systems via null-space-based behavioral control. *Science China Information Sciences*, 59(1), 1-11.

Edwards, W. (1965). Optimal strategies for seeking information: models for statistics, choice reaction times, and human information processing. *Journal of Mathematical Psychology*, 2(6), 312-329.

Gao, J., and Lee, J. D. (2006). Extending the decision field theory to model operators' reliance on automation in supervisory control situations. *IEEE Transactions on Systems, Man, and Cybernetics-Part A: Systems and Humans*, 36(5), 943-959.

Goodrich, M. A., and Schultz, A. C. (2008). Human-robot interaction: a survey. *Foundations and Trends in Human-Computer Interaction*, 1(3), 203-275.

Huang, J., Zhou, N., and Cao, M. (2019a). Adaptive fuzzy behavioral control of second-order autonomous agents with prioritized missions: theory and experiments. *IEEE Transactions on Industrial Electronics*, 66(12), 9612-9622.

Huang, J., Wu, W., Ning, Y., Zhou, N., and Xu, Z. (2019b). A behavior control scheme for multi-robot systems under human intervention. *2019 Chinese Control Conference*, 6189-6193.

Hitsuda, M. (1968). Representation of Gaussian processes equivalent to Wiener process. *Osaka Journal of Mathematics*, 5(2), 299-312.

Musić, S., and Hirche, S. (2017). Control sharing in human-robot team interaction. *Annual Reviews in Control*, 44(2), 342-354.

Milosavljevic, M., Malmaud, J., Huth, A., Koch, C., and Rangel, A. (2010). The drift diffusion model can account for the accuracy and reaction time of value-based choices under high and low time pressure. *Neural Computation*, 5(6), 437-449.

Pentland, A., and Liu, A. (1999). Modeling and prediction of human behavior. *Neural Computation*, 11(1), 229-242.

Peters, J. R., Srivastava, V., Taylor, G. S., Surana, A., Eckstein, M. P., and Bullo, F. (2015). Human supervisory control of robotic teams: integrating cognitive modeling with engineering design. *IEEE Control Systems Magazine*, 35(6), 57-80.

Ren, W., and Beard, R. W. (2008). Distributed consensus in multi-vehicle cooperative control. *Springer*.

Ratcliff, R. (1978). A theory of memory retrieval. *Psychological Review*, 85(2), 59-82.

Ratcliff, R., and McKoon, G. (2008). The diffusion decision model: theory and data for two-choice decision tasks. *Neural Computation*, 20(4), 873-922.

Ratcliff, R., Gomez, P., and McKoon, G. (2004). A diffusion model account of the lexical decision task. *Psychological Review*, 111(1), 159-182.

Ratcliff, R., and Rouder, J. N. (1998). Modeling response times for two-choice decisions. *Psychological Science*, 9(5), 347-356.

Sheridan, T. B. (2016). Human-robot interaction: status and challenges. *Human Factors*, 58(4), 525-532.